Journal Pre-proof


# Compartment-specific effect of sulfamethoxazole at low μg/L concentrations on microbial nitrogen assimilation in a river system

Sarah Haenelt , Caglar Akay , Hans-Hermann Richnow , Steffen Kümmel , Hryhoriy Stryhanyuk , Jochen A. Müller , Niculina Musat

PII: S2589-9147(25)00089-1
DOI: https://doi.org/10.1016/j.wroa.2025.100390
Reference: WROA 100390

To appear in: *Water Research X*

Received date: 24 March 2025
Revised date: 23 July 2025
Accepted date: 27 July 2025

Please cite this article as: Sarah Haenelt , Caglar Akay , Hans-Hermann Richnow , Steffen Kümmel , Hryhoriy Stryhanyuk , Jochen A. Müller , Niculina Musat , Compartment-specific effect of sulfamethoxazole at low μg/L concentrations on microbial nitrogen assimilation in a river system, *Water Research X* (2025), doi: https://doi.org/10.1016/j.wroa.2025.100390

**Highlights**

- Sulfamethoxazole (SMX) increased microbial N assimilation up to 64 % in river samples
- The increase in N assimilation was typically in the order 10 > 100 > 1000 µg/L SMX
- Response to SMX was stronger in samples from near-pristine site than in wastewater-impacted site
- NanoSIMS analysis revealed SMX-dependent N assimilation heterogeneity in microbial community

# Compartment-specific effect of sulfamethoxazole at low μg/L concentrations on microbial nitrogen assimilation in a river system

**Sarah Haenelt[1], Caglar Akay[2,3], Hans-Hermann Richnow[1], Steffen Kümmel[1], Hryhoriy Stryhanyuk[1], Jochen A. Müller[4*], Niculina Musat[5*]**

[1] Department of Technical Biogeochemistry, Helmholtz Centre for Environmental Research, Leipzig, Germany

[2] Department of Molecular Environmental Biotechnology, Helmholtz Centre for Environmental Research, Leipzig, Germany

[3] Department of Exposure Science, Helmholtz Centre for Environmental Research, Leipzig

[4] Institute for Biological Interfaces (IBG 5), Karlsruhe Institute of Technology, Eggenstein-Leopoldshafen, Germany

[5] Department of Biology, Section for Microbiology, Aarhus University, Aarhus, Denmark

***Correspondence:**
Niculina Musat
niculina.musat@bio.au.dk

Jochen A. Müller
jochen.mueller@kit.edu

**Keywords:** riverine microbial community; flume system; antimicrobials; PNEC; microbial activity; NanoSIMS

**Abstract**

Sulfamethoxazole (SMX) is one of the most frequently detected antibiotics in rivers, with concentrations occasionally exceeding the predicted no-effect concentration (PNEC). The impact of such concentrations on the microbial activity of riverine microbial communities remains poorly studied. Here, we investigated the effect of SMX concentrations at the upper end of reported PNEC values (12.5 µg/L) on microbial communities in flume systems with either near-pristine or wastewater-impacted river water. Using a combination of microbiological and chemical methods, we found that SMX was persistent in both near-pristine and wastewater-impacted river water over a time course of 63 days, and had no significant impact on the planktonic bacterial community composition. However, there was an increase in microbial activity after SMX addition. Tracking $^{15}N$ incorporation in both sample types using Nanoscale Secondary Ion Mass Spectrometry (NanoSIMS) and an Elemental Analyser - Isotope Ratio Mass Spectrometer (EA-IRMS) revealed that SMX concentrations in the test range (10, 100 and 1000 µg/L) enhanced nitrogen assimilation from ammonium up to 64 %. The highest increase was found almost always at 10 µg/L SMX. The response was stronger in samples from the near-pristine site compared to the wastewater-impacted site, and in planktonic biomass compared to biofilms. Overall, our findings reveal a transient increase in microbial nitrogen assimilation with environmentally relevant concentrations of SMX in a habitat-specific manner, but not of SMX degradation, which could be of significance for nutrient dynamics and primary productivity in impacted rivers.



## 1. Introduction

Antibiotics are notorious organic micropollutants found in freshwater environments worldwide (Schwarzenbach et al., 2006). Major sources of these compounds in surface waters are raw sewage and effluent from wastewater treatment plants (WWTPs) (Kovalakova et al., 2020; Straub, 2016). Sulfonamides, especially sulfamethoxazole (SMX), are among the most frequently detected antibiotics in impacted rivers owing to their widespread use as inhibitors of bacterial folate biosynthesis and their high chemical stability (Wilkinson et al., 2022). In European rivers, for example, SMX has been detected mostly in the ng/L range, but can reach low µg/L concentrations (Carvalho and Santos, 2016).

Given the ubiquity of SMX, it is important to better understand its impact on aquatic microbial communities as essential contributors to ecosystem functioning (Brandt et al., 2015). Several concentration-dependent effects of SMX have been reported. In meso- and macrocosms, an increase in sulfonamide resistance genes was observed at 4 to 5 µg/L SMX, while concentrations ≤1 µg/L had no apparent effect (Borsetto et al., 2021; Knecht et al., 2022; Vila-Costa et al., 2017). The higher values are close to the predicted no-effect concentration for resistance selection ($PNEC_{resistence}$) of 16 µg/L, estimated with data from clinical bacterial isolates (Bengtsson-Palme and Larsson, 2016). There is less clarity about various other effects of SMX on aquatic microorganisms, with even inconsistent results between studies. Single-species tests revealed high toxicity of SMX towards cyanobacteria, algae, and ammonium oxidizing bacteria (Grenni et al., 2019; Kovalakova et al., 2020; Välitalo et al., 2017; Zhang et al., 2022), with a proposed $PNEC_{toxicity}$ of 0.6 µg/L (Le Page et al., 2017; Straub, 2016). In contrast, studies with communities found no toxicity (Schuijt et al., 2024) or even a stimulatory effect (Duarte et al., 2023; Kergoat et al., 2021) on cyanobacteria at low µg/L concentrations. Furthermore, various effects of SMX up to low µg/L concentrations on the heterotrophic bacterial community have been reported. The list of effects include increases in total nitrogen removal rates (Liu et al., 2024) but also lower denitrification rates (Xu et al., 2020), enhanced aerobic respiration and beta-glucosidase activity (Pesce et al., 2021), expression changes of genes related to N, C, and P cycling (Yergeau et al., 2012), reduced biomass yield (Paumelle et al., 2021), and shifts in community composition (Kergoat et al., 2021). In light of this range of responses, it has been challenging to derive a coherent theme regarding the effects of SMX on microbial processes in aquatic environments.

To address this, we investigated the effect of SMX on river-derived microbial communities using a combination of flume systems, which mimic natural riverine conditions (Borsetto et al., 2021), and batch culture incubations. Sample source was the Holtemme, a small river in Germany investigated previously (Weitere et al., 2021; Haenelt et al., 2023a; Haenelt et al., 2023b). Next to recording standard water quality parameters, we tracked active microorganisms by stable isotope probing (SIP) with $^{15}NH_4^+$ as anabolic substrate (Musat et al., 2014, 2016). $^{15}N$ incorporation with and without added SMX was recorded in planktonic and biofilm-forming microbial communities by Nanoscale Secondary Ion Mass Spectrometry (NanoSIMS) and using an Elemental Analyser - Isotope Ratio Mass Spectrometer (EA-IRMS). We found that SMX increased nitrogen assimilation at low to medium µg/L concentrations, with the effect varying by sample source and exhibiting heterogeneity within microbial communities. These findings provide further evidence that SMX can influence biogeochemical cycles

at environmentally relevant concentrations. Furthermore, we suggest that inter- and intra-sample heterogeneity may explain previously observed variation in community responses.

## 2. Results and Discussion

### 2.1 Flume systems: Long-term experiment over 63 days

To simulate river conditions, we established six flume systems in a climate chamber (17 °C, 16 h light and 8 h dark cycle) using 40 L of water collected from either of two sampling sites at the Holtemme (**Figure S1A**). One site was in the near-pristine part in the Harz Mountains (referred to hereafter as NP for near-pristine), while the second site was located 8 km downstream of the first WWTP discharging into the river (hereafter WI for wastewater-impacted). For each site, one system served as control and two systems were amended once with 12.5 µg/L of $^{12}$C-SMX or $^{13}$C-SMX, with the latter to test for microbial assimilation of SMX-derived carbon (**Figure S1B**).

In the four systems spiked with SMX, the concentration decreased to approximately 8 µg/L on day 8, after which it remained essentially constant until the end of the experiment (**Figure S2A**). In all systems, the $^{13}$C content in microbial biomass samples was at the natural abundance of 1.1% throughout the experiment according to EA-IRMS analysis (**Figure S2B**). Therefore, SMX-derived C assimilation (if any) was below the detection limit. The comparatively short period of eight days during which there was a decrease in SMX concentration also suggest that co-metabolic and abiotic transformation processes occurred at negligible rates (Straub, 2016; Wang and Wang, 2018; Akay et al., 2024). Rather, it is likely that the SMX concentration stabilized after sorption to plastic surfaces and organic matter in the flume systems (Guo et al., 2019). Similarly, Borsetto et al. (2021) observed an initial decrease in SMX concentration starting at 1.2 µg/L in flume systems with surface water and sediment collected downstream of a WWTP, followed by an increase over 24 days. The authors concluded that biodegradation was unlikely in the initial phase. The water in our systems was fully oxygenated, and although bacteria that aerobically degrade SMX are known, degradation does not readily occur under such conditions (Ingerslev and Halling-Sørensen, 2000; Jiang et al., 2014; Ricken et al., 2013). Aerobic SMX degraders may not have been present or only in very small numbers in the Holtemme water, potentially because the SMX concentration in its principal source, the WWTP effluent, is in the low ng/L range and may not be a significant carbon and energy source in the river (Haenelt et al., 2023a; Haenelt et al., 2023b; Švara et al., 2021).

However**,** there was evidence that SMX influenced microbial activities in the flume systems. **Figure 1** shows the dynamics of $NO_3^-$-N, total carbon (TC), total organic carbon (TOC), dissolved carbon (DC), dissolved organic carbon (DOC), and pH in the six systems. While the values for the parameters did not differ substantially in the three WI systems, the NP systems exhibited notable differences depending on the presence or absence of added SMX. In the two NP systems with SMX, the $NO_3^-$-N concentration decreased from a mean of 1.1 mg/L on day 0 to below the limit of quantification (0.042 mg/L) within 21 days, whereas it took over 40 days without SMX addition. $NH_4^+$-N and $NO_2^-$-N concentrations were below 0.1 mg/L in all six systems, with no apparent differences (not shown). It seems more likely that the faster nitrate removal was due to increased assimilation rather than a higher dissimilatory nitrate reduction rate under full oxygen saturation.

The literature provides a contrasting picture of the effect of low concentrations of SMX on nitrate turnover: (i) a slight increase in denitrification was described for microcosms with Morcille River sediment and 5 µg/L SMX (Pesce et al., 2021), (ii) inhibition of denitrification was measured in Yarlung Zangbo River sediment slurries with SMX > 1 µg/L (Xu et al., 2020), and (iii) lower nitrate concentrations but also lower denitrification rates were recorded in Yangtze River sediment slurries with SMX in the range of 29-57 ng/L (Chen et al., 2021). The reasons for these apparent discrepancies are unknown and could be the result of differences in the composition of the microbial community and in SMX concentration and bioavailability due to different sediment types with various sorption capacity (Hou et al., 2010).

Here, TC, TOC, DC, and DOC increased in all six flume systems over time, presumably due to photosynthetic activity, as evidenced by the formation of a thin algal or cyanobacterial film on the inner walls of the systems. After day 21, these parameters exhibited a greater increase in the NP system without added SMX compared to the NP systems with SMX. The lower accumulation of organic carbon in the presence of SMX may be attributed to the inhibition of primary productivity. SMX is acutely and chronically toxic to aquatic photosynthetic microorganisms (Kovalakova et al., 2020; Zhang et al., 2022), with long-term inhibition occurring at or below (depending on test species and exposure time) the SMX concentration in our flume systems. The underlying mechanisms for the comparably high sensitivity of aquatic photosynthetic organisms are not yet clear, and may be multifactorial and may involve general stress response systems (Zhang et al., 2022). Here, SMX did not affect the relative abundance of *Cyanobacteria* and chloroplasts in the water according to amplicon sequencing (Section 2.1.2). However, absolute abundances were not quantified, and the composition

of biofilms that developed in the systems were not characterized. Uneven biofilm distribution, according to visual inspection and predictably influenced by flume geometry and light source positioning, would have prevented accurate extrapolation of discrete sample data. Alternatively or concomitantly to an effect on photosynthetic microorganisms, the lower accumulation of organic carbon in the SMX-amended systems could have been due to increased aerobic respiration as in the aforementioned flume systems containing Morcille River sediment (Pesce et al., 2021).

### 2.1.2 Bacterial community structure

To investigate whether the different activity patterns were due to shifts in bacterial community composition induced by SMX, we performed 16S rRNA gene amplicon sequencing on water samples from the six NP and WI flume systems. A total of 8.2 million high-quality read pairs were generated from 44 samples (131k to 269k read pairs per sample). Patterns in alpha and beta diversities did not provide evidence for an influence of SMX on bacterial community structure (**Figure S3)**. At both sampling site types, the majority of amplicon sequence variants (ASVs) affiliated with typical bacterial inhabitants of an oxic river (**Table S1**). Predominant families were *Alcaligenaceae, Burkholderiaceae, Caulobacteraceae Comamonadaceae, Flavobacteriaceae, Legionellaceae* and *Sphingomonadaceae*. SMX had no effect on the prevalence of the 20 most abundant bacterial families. ASVs associated with *Cyanobacteria* other than chloroplasts had a total relative abundance of approximately 1% in WI and 1.8% in NP samples, respectively. Their abundance declined over time, with no substantial differences between the flume systems. Similar findings have been reported previously, where bacterial community compositions in flume systems remained unaffected by the presence of 4 µg/L SMX (Borsetto et al., 2021).

### 2.1.3 Ammonium assimilation by the microbial communities

We analyzed bulk microbial activity in samples from all flume systems by tracking the incorporation of $^{15}N$ from labeled ammonium into biomass over 24 h using EA-IRMS. **Figure 2** shows that $^{15}N$ isotope enrichment relative to natural abundance [x($^{15}N$) in percent] were higher in the systems with SMX. Most prominently, x($^{15}N$) increased to 18.6% and 20.6% in the two WI samples with SMX in samples from day 0, compared to 7.1% in the system without SMX – a 64% increase in isotope enrichment with SMX. Across the remaining seven sampling days, the general trend showed higher x($^{15}N$) values in the presence of SMX. In WI water systems, x($^{15}N$) was 9.1% to 31% higher with SMX (mean increase of 18.1%) during five sampling days (days 8, 21, 28, 42, and 63). On the remaining two sampling days (days 3 and 14), the differences were within the variability of the replicates. In the

NP water systems, x($^{15}$N) was elevated in all but one samples (day 28 with $^{12}$C SMX), with increases ranging from 5.0% to 40.5% in the presence of SMX compared to without the antibiotic (mean increase of 21 %).

Therefore, there was evidence for SMX affecting microbial activities but not community composition in the systems. The most pronounced effect was observed for nitrogen assimilation, with the extent of the response varying depending on the sample origin. We acknowledge that there were only two replicate flume systems with SMX and one control per sampling site, which necessitates cautious interpretation of these findings . However, our findings align with previous reports demonstrating that low µg/L concentrations of SMX can stimulate microbial activity (Cui et al., 2020; Kergoat et al., 2021; Liu et al., 2017; Paumelle et al., 2021; Pesce et al., 2021). To further investigate the effect of SMX on microbial activity in Holtemme water, we opted for short-term microcosm experiments with fresh samples.

### 2.2 Batch cultivation: Short-term experiment over 24 hours

#### 2.2.1 Bulk analysis using EA-IRMS

We incubated surface water and biofilm samples collected from NP and WI with SMX concentrations of 10, 100 and 1000 µg/L, representing the high range of SMX detected in rivers (Larsson, 2014; Wilkinson et al., 2022), and determined x($^{15}$N) by EA-IRMS. Across all sample types, x($^{15}$N) values were 11.2% to 37.6% higher in the presence of 10 or 100 µg/L SMX compared to the corresponding SMX-free incubation (**Figure 3)**. Water samples exhibited greater $^{15}$N enrichment than biofilm samples, with x($^{15}$N) values ranging from 7.1% to 28.1% for NP and 9.9% to 17.9% for WI samples. In biofilm samples, x($^{15}$N) values ranged from 3.4% to 6.3% for NP and 5.3% to 9.7% for WI samples. Previous findings showed that biofilm-associated cells are often less metabolically active than planktonic cells, likely due to nutrient and oxygen limitations (Crabbé et al., 2019). Additionally, extracellular polymeric substances in the biofilm may have hindered the diffusion of $^{15}$N-labeled ammonium, limiting its assimilation. In NP and WI biofilm, the greatest increase in x($^{15}$N) occurred at 10 µg/L SMX, whereas enrichment continued to rise in WI river water samples at 100 µg/L SMX, suggesting that the WI microbial community was more adapted to the antibiotic. At 1000 µg/L SMX, no further increase in N assimilation was observed, and x($^{15}$N) values even declined in the NP biofilm, possibly due to an inhibitory effect of SMX counteracting any enhancement of ammonium assimilation.

### 2.2.2 Quantifying ammonium assimilation using NanoSIMS

To capture cellular heterogeneity of the SMX effect on ammonium assimilation, we carried out NanoSIMS analysis with surface water and biofilm samples from the NP and WI sites (**Figure 4**). $^{15}N$ assimilation is shown as violin plots (**Figure 5)**, expressed as atom % enrichment ($K_f$) calculated after adjusting for the effects of sample preparation (Stryhanyuk et al., 2018). Klicken Sie hier, um Text einzugeben.

The shape of the violin plots revealed three main differences in assimilation activity with and without SMX. First, there was an increase in $K_f$ in all samples in the presence of SMX. The highest increase was with 10 µg/L SMX, except in WI biofilm samples, where the median $K_f$ were similar at 10 µg/L and 1000 µg/L SMX. Across all four sample types, the mean $K_f$ was 19.6% - 36.1% higher at 10 µg/L SMX compared to treatments without the antibiotic. This pattern mirrored the results of the bulk measurements, except in WI surface water, where 100 µg/L SMX had the strongest effect instead of 10 µg/L, possibly due to structural and functional heterogeneity among the analyzed samples.

Second, ammonium assimilation was heterogeneously distributed within each community, and this heterogeneity varied by sample source. Without SMX, the highest heterogeneity was observed in WI surface water samples, possibly because a less-active fraction of the microbial community consisted of wastewater-derived cells not yet adapted to the river environment.

Third, surface water samples exhibited higher median $K_f$ values (51.6 at% – 78.3 at%) than corresponding biofilm samples (6.8 at% – 21.6 at%), consistent with the bulk analysis results. In surface water samples, nearly all analyzed biomass responded to SMX. In contrast, in biofilm samples, a substantial fraction of the biomass either did not respond or experienced SMX-induced inhibition, which counteracted any increase in $^{15}N$ assimilation activity.

### 2.3.2 Mechanistic considerations, limitations, and outlook

The underlying mechanism driving this increased N assimilation is uncertain. In the literature, a so-called hormetic effect of SMX and other sulfonamides at low µg/L concentrations has been proposed, characterized by a biphasic dose-response where low concentrations stimulate and high concentrations inhibit (Li et al., 2020; Liu et al., 2017; Sun et al., 2019 Wang et al., 2016; You et al., 2016). Low SMX concentrations would promote ATP and macromolecule synthesis, ultimately enhancing cell proliferation. Sulfonamides may bind to the LuxR regulator, inducing transcriptional changes that lead to increased growth (Lin et al., 2023). This model is in line with reports that low SMX concentrations

increase (i) bioluminescence in *Aliivibrio fischeri*, which is under LuxR control (Vasconcelos et al., 2017), (ii) aerobic respiration in investigated freshwater sediments (Pesce et al., 2021), and (iii) conjugation transfer frequency (Sun et al., 2019). Thus, SMX would act as signaling molecule at low, sub-inhibitory concentrations, a function proposed for various antibiotics (Fajardo and Martínez, 2008). It should be noted that it would be a coincidental rather than an evolved function since sulfonamides are synthetic antimicrobials, not naturally produced antibiotics. A qualifier to these studies is that microbial growth assessments were based on optical density measurements in microtiter plates, which can be confounded by biofilm formation on well surfaces (Vesterlund et al., 2005). Biofilm formation under antibiotic stress is well documented, and would be consistent with an involvement of LuxR in the bacterial response to SMX. Instead of net growth stimulation, an alternative explanation may be an increased biomass turnover due to cellular stress induced by SMX exposure.

In this study, we did not quantify bacterial growth or cell status indicators, as we did not consider it reliable extrapolating results from discrete samples to the total biofilm mass in the flume systems in the 63-day experiment and accurately tracking respective changes on pebble surfaces over the 24-h experimental period. Moreover, given the heterogeneous ammonium assimilation rates revealed by the NanoSIMS analysis, bulk measurements may not provide further clarity on the effects of low-doses of SMX on microbial communities. A more promising approach could involve nucleic acid- and protein-SIP using $^{15}$N-labelled ammonium or nitrate, allowing the identification of bacteria particularly responsive to low doses of SMX and illuminate the cellular processes involved. Further studies are also needed to better define the effects of chronic and peak SMX exposure on photosynthetic activities in impacted rivers, and to test SMX concentrations below 10 µg/L for their impact on ammonium assimilation.



## 3. Conclusions

This study demonstrates that environmentally relevant concentrations of SMX stimulate microbial nitrogen assimilation in river water, with potentially significant implications for nutrient cycling and ecosystem function. Our integrated approach, employing flume systems and batch experiments coupled with SIP using EA-IRMS and NanoSIMS, consistently revealed enhanced nitrogen uptake, ranging from a two-fold increase in nitrate transformation to 10-64% higher ammonium assimilation. The concurrent reduction in aqueous carbon content suggests a complex metabolic shift induced by SMX

exposure. Heterogeneity in response observed within and across samples, revealed by NanoSIMS analysis, likely explains inconsistencies in previous studies using communities from diverse habitats and locations. Promising future research directions include identifying the specific bacterial taxa responsible for these effects, providing a basis for investigating the cellular mechanisms that mediate the observed changes in nitrogen assimilation, and assessing the broader ecological consequences of SMX-induced shifts in nutrient cycling.

## 4. Materials and Methods

### 4.1 Long-term experiment with flume systems

#### 4.1.1 Flume system setup

The six flume systems were established in a climate chamber located at the Helmholtz Centre for Environmental Research in Magdeburg, Germany. The flumes were constructed from polycarbonate and had dimensions of 140 cm × 15 cm × 20 cm. They were connected to HDPE drums equipped with Red Dragon 5 ECO pumps (Royal Exclusive, Germany) using HDPE and PVC pipes. These pumps were used to recirculate the water in the system (10 L/min). The ambient temperature was maintained at 17 °C according to the water temperature at the wastewater-impacted site at the time of sampling. Water temperature at the near-pristine site was slightly lower, measuring 15 °C. Artificial lighting was provided with a 16 h light and 8 h dark cycle (Econlux Solarstinger SunStrip 800 mm, Germany). Water was collected from two sites at the 47-km long Holtemme river in Saxony-Anhalt, Germany (**Figure S1A**). The river originates in the Harz National Park and is considered nearly pristine in the upper mountainous part, where the stream bed has not been anthropogenically altered and only traces of a limited number of anthropogenic pollutants, such as the insecticide diethyltoluamide, have been found (Weitere et al., 2021). Downstream from the mountains, the landscape is dominated by agriculture. The Holtemme passes through several small cities (≤ 32,000 inhabitants) and receives wastewater from two WWTPs before draining into the Bode river. The first water collection site was in the near-pristine part in the Harz Mountains (51°49'00.9"N 10°43'28.6"E), while the second site was located 8 km downstream of the first WWTP discharging into the Holtemme in an area dominated by agriculture (51°53'05.8"N 10°57'47.5"E). Samples from these sites and respective flume systems will be referred to hereafter as NP for near-pristine and WI for wastewater-impacted. Six flume systems were filled with 40 L of river water each, three from the NP and three from the WI site. Two systems

each from NP and WI were spiked once with either 12.5 µg/L $^{12}$C-SMX or 12.5 µg/L $^{13}$C-SMX [2 mL of 250 mg/L solution in equal volumes of methanol and double-distilled $H_2O$ ($ddH_2O$)], while the remaining two flume systems were used as control (**Figure S1B**). The flume systems were operated under these conditions for 63 days.

### 4.1.2 Sampling and sample preparation

Water samples were collected from the flume systems at eight different time points (day 0, 3, 8, 14, 21, 28, 42, and 63) during the experiment. On each sampling day except day 0, we took multiple water samples from all six systems: 500 mL for DNA extraction, 1.5 mL for measuring total carbon (TC) and total organic carbon (TOC), 1.5 mL of filtered water for measuring dissolved carbon (DC) and dissolved organic carbon (DOC), and 60 mL of filtered water for measuring ammonium ($NH_4^+$-N), nitrite ($NO_2^-$-N) and nitrate ($NO_3^-$-N) concentrations. Filtration was performed using PSE PALL filters (diameter 47 mm, pore size 0.22 µm, Pall Corporation, NY USA) and a vacuum system. On day 0, the samples were directly taken from the river water. In addition, 1 mL of filtered water was collected for LC-MS/MS analysis on all sampling days from the flume systems spiked with SMX. For the two control systems, samples for LC-MS/MS were collected only on days 0 and 63. On each sampling day, 50 mL water samples from all six flume systems were spiked with 800 µL $^{14}NH_4Cl$ and 200 µL $^{15}NH_4Cl$ each (both stocks at a concentration of 100 mM) and incubated at RT and 20 rpm for 24 h prior to filtration and further analysis with an EA-IRMS as described in detail below.

### 4.1.3 Chemical analyses

Water temperature, pH, and oxygen saturation were measured in all flume systems on each sampling day using a MultiLine® Multi 3630 IDS multi-parameter portable meter, equipped with a SenTix 940 pH electrode and an FDO 925 IDS oxygen probe (all from Xylem Analytics, Germany). Concentrations of TC, TOC, DC and DOC were quantified using a multi N/C 2100S Analyzer (Analytic Jena, Germany). $NH_4^+$-N, $NO_2^-$-N, and $NO_3^-$-N concentrations were determined using a SanSERIES Continuous-flow Analysator (Skalar, The Netherlands) at the Central Laboratory for Water Analytics and Chemometrics of the Helmholtz Centre for Environmental Research Magdeburg.

For LC-MS/MS analysis, stock solutions of 10 mg/L of $^{12}$C-SMX and $^{13}$C-SMX, respectively (Sigma-Aldrich, MO, USA) were stored in pure methanol at -20 °C. Prior to the measurement, standards with 0.01, 0.02, 0.05, 0.075, 0.1, 0.2, 0.5, 0.75, 1, and 2 µg/L SMX plus 0.1 µg/L SMX-$D_4$ as internal standard were prepared in 900 µL $H_2O$ with 0.1 % formic acid and 100 µL of methanol. The

concentrations of $^{12}$C-SMX and $^{13}$C-SMX were measured using an Agilent 1260 Infinity II Series liquid chromatography (LC; Agilent Technologies, CA, USA) system coupled to an AB Sciex QTRAP® 6500+ tandem mass spectrometer (MS/MS) equipped with a Turbo V™ ion source (AB Sciex, UK). The multiple reaction monitoring (MRM) mode was used with electrospray ionization in positive polarity. The separation of analytes was carried out with a Zorbax Eclipse Plus Rapid Resolution HT-C18 column (100 mm × 3.0 mm, 1.8 µm; Agilent Technologies, CA, USA) attached to a Phenomenex Security guard cartridge system (C18, ODS, Octadecyl; Phenomenox, CA, USA) operated at 30 °C. The injection volume and the flow rate were set at 50 µL and 0.4 mL/min, respectively. The binary mobile phase consisted of 0.2 % formic acid in LC-MS grade $H_2O$ (solvent A) and methanol (solvent B). The LC gradient program started with a 2-min equilibration at 10 % B, followed by a 1-min linear increase to 60 % B, 5-min linear increase to 90 % B, 3-min hold at 90 % B, 0.1-min decrease to 10 % B, and 4.9-min hold at 10 % B. The dwell time of the analytes was 40 ms. The ion source-dependent MS parameters were kept constant during the whole acquisition: Curtain Gas (CUR): 35 psi; Ion spray voltage (IS): 5000 V; Turbo Spray Temperature (TEM): 450 °C; Nebulizer Gas (GS1): 60 psi; Heater gas (GS2): 60 psi; CAD Gas: Medium. Nitrogen was used as the curtain and collision gas. The compound-dependent MS parameters were optimized by direct infusion of the analytes of interest (**Table S2**). All data were acquired and processed using Analyst 1.7.2 Software (Sciex, MA, USA).

For EA-IRMS analysis of $^{13}$C and $^{15}$N incorporation of into microbial biomass, water samples were filtered through pre-combusted (5 h at 450 °C) 25-mm glass microfiber filters, grade GF/F (Whatman, UK), rinsed with 10 mL Milli-Q water, and dried under vacuum for 10 min at RT. The filters were placed in a desiccator with a tray of 6N hydrochloric acid (Carl Roth, Germany) underneath for overnight decalcification. Then, the filters were cut in half, each half wrapped in 10 × 10 mm tin capsules (HEKAtech, Germany) and analyzed using a Flash 2000 Organic Elemental Analyzer (EA), coupled with a ConFlo IV open split system to a Delta V Advantage isotope ratio mass spectrometer (all Thermo, Germany). Flash combustion was performed at 1020 °C by providing an oxygen pulse of 12.5 mL/min in a combustion reactor filled with silvered cobalt oxide, chromium oxide (both IVA Analysentechnik, Germany), and quartz wool (HEKAtech, Germany). The oxidation products were transferred in a helium carrier gas flow of 120 L/min to the reduction oven, filled with reduced copper (HEKAtech) and maintained at 650 °C. Remaining water was trapped with magnesium perchlorate (HEKAtech) and the gas mixture was separated on an IRMS separation column (length 300 cm, OD 6 mm, ID 5 mm) operated at 50 °C. The $^{13}$C and $^{15}$N enrichments were expressed in atom fraction x($^{i}$E)

as suggested by Coplen (2011). The atom fraction x($^{i}$E) is calculated using the amount of isotope $^{i}$E and isotope $^{j}$E of an element E (Equation 1).

$$x(\ ^{i}E) = \frac{n(\ ^{i}E)}{n(\ ^{i}E) + n(\ ^{j}E)} Eq.1$$

#### 4.1.4 Bacterial community analysis

DNA extraction, 16S rRNA gene amplicon sequencing, and data analysis were conducted as previously described (Haenelt et al., 2023b; Knecht et al., 2022). In brief, biomass was removed from the PSE Pall filters by agitating the filters with zirconium beads in BE buffer, and DNA extraction was conducted using a NucleoSpin Microbial DNA Kit (Macherey Nagel, Germany) following the manufacturer's protocol. A 16S rRNA gene amplicon library was prepared with PCR primers targeting the variable region V3 of the 16S rRNA gene. The libraries were generated with an Illumina NextSeq 500/550 High Output Kit v2.5 and sequenced on an Illumina Nextseq-System (Illumina, San Diego, CA, USA). Data analysis was carried out with the software package QIIME 2 (Bokulich et al., 2018; Bolyen et al., 2019) and DADA2 (Callahan et al., 2016). Taxonomic assignments were carried in QIIME 2 using the pre trained classifier "Silva 138 99% OTU full-length sequences", and manually curated in R using phyloseq (McMurdie and Holmes, 2013). Alpha diversity was assessed by computing the Observed Richness and Shannon diversity indices. For beta diversity, a non-metric multidimensional scaling (NMDS) plot was built from Bray Curtis dissimilarities using the R package vegan, version 2.6-4 (Oksanen et al., 2022).

### 4.2 Short-term isotope labelling experiment over 24 hours

#### 4.2.1 Experimental set-up

To investigate the short-term effect of SMX on nitrogen assimilation by planktonic and biofilm microbial communities, we employed EA-IRMS and NanoSIMS analysis. Surface water and pebbles with attached biofilm were collected from the two sites, NP and WI, in sterile and pre-rinsed 250-mL glass bottles. Water volumes of all setups are provided in **Table S3**. SMX was added at concentrations of 10, 100 and 1000 µg/L, prepared from a 250 mg/L stock solution in dd$H_2O$. Negative controls did not receive SMX. SIP using $^{15}$N-labeled ammonium as a general metabolic tracer was applied to quantify microbial N assimilation. 500 mM $^{15}NH_4Cl$ and 500 mM $^{14}NH_4Cl$ (125 to 500 µL depending on the water volume) were added to all samples to reach a final concentration of 3.1 mM each. For planktonic cells, surface water was collected from the river directly and amended with $^{15}$N-ammonium

and $^{13}$C-SMX. For biofilm samples, river water was filtered using 0.45 µm PES syringe filters (Whatman, UK) to remove planktonic cells, and three pebbles were added to the glass bottle prior to amendment with SMX and ammonium.

All bottles were incubated for 24 hours at natural light conditions with shaking at 80 rpm. At time points 0 and 24 hours, 1 mL of water was collected from each bottle for SMX concentration measurements. Measured SMX concentrations agreed with calculated concentrations, indicating negligible sorption to the glass walls of the bottles or the pebbles.

For bulk analysis via EA-IRMS, water samples (50 mL) were filtered in triplicates and biofilm samples were detached from the pebbles outside the incubation bottles using a metal inoculation loop. Six samples per setup were analyzed as described above (Section 4.1.3).

#### 4.2.2 SIP-NanoSIMS analysis

Assimilation of $^{15}$N-ammonium into microbial biomass was further analyzed using a NanoSIMS 50L instrument (AMETEK, CAMECA, France). Planktonic or biofilm-forming cells from freshly collected samples were incubated with 50 at% of $^{15}$N-ammonium for 24 h as described above. The preparation of the samples for NanoSIMS analysis is described in detail in the Supplemental Material. During analysis, corresponding masses of seven secondary ion species were acquired ($^{16}O^{1}H^{-}$ for sugar signatures; $^{12}C_2^{-}$ and $^{12}C_2{}^{1}H^{-}$ to differentiate between organics of different densities originating from sample carriers, extracellular polymeric substances and biomass; $^{12}C^{14}N^{-}$ as a general intrinsic marker for biomass; $^{12}C^{15}N^{-}$ to assess the assimilation of $^{15}$N-ammonium into biomass; $^{31}P^{-}$ and $^{32}S^{-}$ as intrinsic biomarkers for RNA and proteins, respectively). Measurements were conducted with mass resolving power (MRP) above 8000, 20×140 µm (width × height) nominal size of the entrance slit, 40×1800 µm exit slits, an aperture of 200×200 µm, and an energy slit cutting off 30 % of secondary ions in their energy-distribution tail. Caesium (Cs) pre-implantation was performed in two steps. Low energy 50 eV $Cs^{+}$ ions in a 400 pA beam were deposited over a 100×100 µm$^2$ sample area for 17 min. Then, 16 keV $Cs^{+}$ ions in a 200 pA beam were pre-implanted within the same 100×100 µm$^2$ area for 15 min. Within these pre-implanted areas, 35×35 µm$^2$ fields of view were scanned in a 512×512 pixel raster using a 4 pA primary $Cs^{+}$ ion beam with dwelling time of 2 ms/pixel. To ensure complete sample consumption in each field of view, data acquisition in 80 scans was performed. The acquired data were corrected for lateral drift using the Look@NanoSIMS (LANS) software (Polerecky et al., 2012).

Analysis of nitrogen assimilation in the heterogeneous river samples presented challenges for single-cell isotopic analysis due to the wide range of biomass sizes and structures observed (e.g., filaments, cell fragments (**Figure 4CD**). Calculating a mean N assimilation for entire agglomerates or cells would not accurately reflect the isotopic heterogeneity within these structures. Therefore, we utilized a pixel-based approach to analyze NanoSIMS data. This involved calculating the N assimilation for each individual pixel within defined regions of biomass, effectively treating each pixel as an independent data point. This method allowed us to capture the full range of isotopic values within biomass agglomerates and significantly increased the number of data points.

Microbial cells and biomass aggregates were defined as regions of interest (RoI) based on distribution maps of $^{12}C^{14}N^-$ ions as biomass intrinsic biomarker. The RoI were defined on $CN^-$ ion maps using an automatic thresholding mode, recognizing voxels with $CN^-$ ion counts over 5% of maximal counts as biomass i.e., cell-related. The fraction of assimilated nitrogen was calculated in each voxel within the defined RoI (**Table S4**). The relative nitrogen assimilation $K_f$ was calculated using equation 2 (Stryhanyuk et al., 2018), where $F_f$ refers to the fraction of $^{15}N$ at the final time point after 24 h of incubation, $F_i$ refers to the fraction of $^{15}N$ at the initial time point ($F_i$=0.00364) at natural abundance of $^{15}N$, and $F_S$ is the fraction of $^{15}N$ in the added ammonium ($F_S$=0.5).

$$K_f = \frac{F_f - F_i}{F_s - F_i} = \frac{\frac{^{12}C^{15}N}{^{12}C^{15}N + {}^{12}C^{14}N} - 0.00364}{0.5 - 0.00364} \quad Eq.2$$

### 4.3 Statistical analyses

For statistical analyses, we performed Kruskal-Wallis and Dunn's tests using the R package rstatix, version 0.7.2 (Kassambara, 2023).

### Declaration of Competing Interests

Author HHR is employed by Isodetect Umweltmonitoring GmbH (Leipzig, Germany). The other authors declare that the research was conducted in the absence of any commercial or financial relationships that could be construed as a potential conflict of interest.

### Author Contributions

Conceptualization and Methodology: SH, HHR, JAM, and NM. Investigation: SH. Data curation and Formal analysis: SH, SK, and HS. Methodology: CA. Writing – original draft: SH and JAM. Writing – review and editing: JAM and NM.

**Acknowledgments**

We would like to thank the Helmholtz Centre for Environmental Research for funding this PhD project through the PhD college initiative - FATE (Fate and effects of antibiotics from sources to sinks: Bridging the scale from molecular-level processes to large-scale observations in engineered and natural systems), included in its research program "PoF IV". We sincerely thank Florian Zander, Hans-Joachim Dahlke, Patrick Fink, and Kurt Friese for their invaluable expertise and support throughout the experiments conducted at UFZ Magdeburg. The NanoSIMS analyses were carried out at the ProVIS Centre for Chemical Microscopy, which was established by the European Regional Development Funds (EFRE – Europe funds Saxony) and the Helmholtz Association at the Helmholtz Centre for Environmental Research Leipzig. Special thanks to our colleagues from the Central Laboratory for Water Analytics and Chemometrics at the Helmholtz Centre for Environmental Research Magdeburg, especially Ms. Goreczka, Ms. Butscher and Ms. Hoff as responsible technicians, and to David Thiele and Florian Lenk for Illumina sequencing. Further, we are thankful for the use of the analytical facilities of the Laboratories for Stable Isotopes (LSI) of the Helmholtz Centre for Environmental Research Leipzig. N.M. was funded by the Novo Nordisk Foundation through an NNF Young Investigator Award, grant NNF22OC0071609 ReFuel.

**References**

Akay, C.; Ulrich, N.; Rocha, U.; Ding, C.; Adrian, L. (2024): *Sequential Anaerobic-Aerobic Treatment Enhances Sulfamethoxazole Removal: From Batch Cultures to Observations in a Large-Scale Wastewater Treatment Plant*. Environmental Science and Technology, 58(28), p.12609–12620. https://doi.org/10.1021/acs.est.4c00368.

Benettoni, P.; Ye, J.-Y.; Holbrook, T. R.; et al. (2020): *Surface cleaning and sample carrier for complementary high-resolution imaging techniques*. Biointerphases, 15(2), p.21005. https://doi.org/10.1116/1.5143203.

Bengtsson-Palme, J.; Larsson, D. G. (2016): *Concentrations of antibiotics predicted to select for resistant bacteria: Proposed limits for environmental regulation*. Environment International, 86, p.140–149. https://doi.org/10.1016/j.envint.2015.10.015.

Bokulich, N. A.; Kaehler, B. D.; Rideout, J. R.; et al. (2018): *Optimizing taxonomic classification of marker-gene amplicon sequences with QIIME 2's q2-feature-classifier plugin*. Microbiome, 6(1), p.90. https://doi.org/10.1186/s40168-018-0470-z.

Bolyen, E.; Rideout, J. R.; Dillon, M. R.; et al. (2019): *Reproducible, interactive, scalable and extensible microbiome data science using QIIME 2*. Nature Biotechnology, 37(8), p.852–857. https://doi.org/10.1038/s41587-019-0209-9.

Borsetto, C.; Raguideau, S.; Travis, E.; et al. (2021): *Impact of sulfamethoxazole on a riverine microbiome*. Water Research, p.117382. https://doi.org/10.1016/j.watres.2021.117382.

Brandt, K. K.; Amézquita, A.; Backhaus, T.; et al. (2015): *Ecotoxicological assessment of antibiotics: A call for improved consideration of microorganisms*. Environment International, 85, p.189–205. https://doi.org/10.1016/j.envint.2015.09.013.

Callahan, B. J.; McMurdie, P. J.; Rosen, M. J.; et al. (2016): *DADA2: High-resolution sample inference from Illumina amplicon data*. Nature Methods, 13(7), p.581–583. https://doi.org/10.1038/nmeth.3869.

Carvalho, I. T.; Santos, L. (2016): *Antibiotics in the aquatic environments: A review of the European scenario*. Environment International, 94, p.736–757. https://doi.org/10.1016/j.envint.2016.06.025.

Chen, C.; Yin, G.; Hou, L.; et al. (2021): *Effects of sulfamethoxazole on coupling of nitrogen removal with nitrification in Yangtze Estuary sediments*. Environmental Pollution, 271:116382. https://doi.org/10.1016/j.envpol.2020.116382.

Chen, J.; Yang, Y.; Ke, Y.; et al. (2022): *Anaerobic sulfamethoxazole-degrading bacterial consortia in antibiotic-contaminated wetland sediments identified by DNA-stable isotope probing and metagenomics analysis*. Environmental Microbiology, 24(8), p.3751–3763. https://doi.org/10.1111/1462-2920.16091.

Coplen, T. B. (2011): *Guidelines and recommended terms for expression of stable-isotope-ratio and gas-ratio measurement results*. Rapid Communications in Mass Spectrometry, 25(17), p.2538–2560. https://doi.org/10.1002/rcm.5129.

Crabbé, A.; Jensen, P. Ø.; Bjarnsholt, T.; Coenye, T. (2019): *Antimicrobial Tolerance and Metabolic Adaptations in Microbial Biofilms*. Trends in Microbiology, 27(10), p.850–863. https://doi.org/10.1016/j.tim.2019.05.003.

Cui, M.; Liu, Y.; Zhang, J. (2020): *Sulfamethoxazole and tetracycline induced alterations in biomass, photosynthesis, lipid productivity, and proteomic expression of Synechocystis sp. PCC 6803*. Environmental Science and Pollution Research International, 27(24), p.30437–30447. https://doi.org/10.1007/s11356-020-09327-6.

Duarte, J. A.; Ribeiro, A. K.; Carvalho, P. de; Bortolini, J. C.; Ostroski, I. C. (2023): *Emerging contaminants in the aquatic environment: phytoplankton structure in the presence of sulfamethoxazole and diclofenac*. Environmental Science and Pollution Research International, 30(16), p.46604–46617. https://doi.org/10.1007/s11356-023-25589-2.

Fajardo, A.; Martínez, J. L. (2008): *Antibiotics as signals that trigger specific bacterial responses*. Current Opinion in Microbiology, 11(2), p.161–167. https://doi.org/10.1016/j.mib.2008.02.006.

Grenni, P.; Patrolecco, L.; Rauseo, J.; et al. (2019): *Sulfamethoxazole persistence in a river water ecosystem and its effects on the natural microbial community and Lemna minor plant*. Microchemical Journal, 149, p.103999. https://doi.org/10.1016/j.microc.2019.103999.

Guo, X.; Chen, C.; Wang, J. (2019): *Sorption of sulfamethoxazole onto six types of microplastics*. Chemosphere, 228, p.300–308. https://doi.org/10.1016/j.chemosphere.2019.04.155.

Haenelt, S.; Richnow, H.-H.; Müller, J. A.; Musat, N. (2023a): *Antibiotic resistance indicator genes in biofilm and planktonic microbial communities after wastewater discharge*. Frontiers in Microbiology, 14, p.1252870. https://doi.org/10.3389/fmicb.2023.1252870.

Haenelt, S.; Wang, G.; Kasmanas, J. C.; et al. (2023b): *The fate of sulfonamide resistance genes and anthropogenic pollution marker intI1 after discharge of wastewater into a pristine river stream*. Frontiers in Microbiology, 14, p.1058350. https://doi.org/10.3389/fmicb.2023.1058350.

Hou, J.; Pan, B.; Niu, X.; Chen, J.; Xing, B. (2010): *Sulfamethoxazole sorption by sediment fractions in comparison to pyrene and bisphenol A*. Environmental Pollution, 158(9), p.2826–2832. https://doi.org/10.1016/j.envpol.2010.06.023.

Ingerslev, F.; Halling-Sørensen, B. (2000): *Biodegradability properties of sulfonamides in activated sludge*. Environmental Toxicology and Chemistry, 19(10), p.2467–2473. https://doi.org/10.1002/etc.5620191011.

Jiang, B.; Li, A.; Di Cui; et al. (2014): *Biodegradation and metabolic pathway of sulfamethoxazole by Pseudomonas psychrophila HA-4, a newly isolated cold-adapted sulfamethoxazole-degrading bacterium*. Applied Microbiology and Biotechnology, 98(10), p.4671–4681. https://doi.org/10.1007/s00253-013-5488-3.

Kassambara, A. (2023): *rstatix: Pipe-Friendly Framework for Basic Statistical Tests.*

Kergoat, L.; Besse-Hoggan, P.; Leremboure, M.; et al. (2021): *Environmental Concentrations of Sulfonamides Can Alter Bacterial Structure and Induce Diatom Deformities in Freshwater Biofilm Communities*. Frontiers in Microbiology, 12, p.643719. https://doi.org/10.3389/fmicb.2021.643719.

Knecht, C. A.; Krüger, M.; Kellmann, S.; et al. (2022): *Cellular stress affects the fate of microbial resistance to folate inhibitors in treatment wetlands*. Science of the Total Environment, 845, p.157318. https://doi.org/10.1016/j.scitotenv.2022.157318.

Kovalakova, P.; Cizmas, L.; McDonald, T. J.; et al. (2020): *Occurrence and toxicity of antibiotics in the aquatic environment: A review*. Chemosphere, 251, p.126351. https://doi.org/10.1016/j.chemosphere.2020.126351.

Larsson, D. J. (2014). *Pollution from drug manufacturing: review and perspectives*. Philosophical Transactions of the Royal Society B: Biological Sciences, 369(1656), p. 20130571. https://doi.org/10.1098/rstb.2013.0571

Le Page, G.; Gunnarsson, L.; Snape, J.; Tyler, C. R. (2017): *Integrating human and environmental health in antibiotic risk assessment: A critical analysis of protection goals, species sensitivity and antimicrobial resistance*. Environment International, 109, p.155–169. https://doi.org/10.1016/j.envint.2017.09.013.

Li, X.; Shi, J.; Sun, H.; Lin, Z. (2020): *Hormetic dose-dependent response about typical antibiotics and their mixtures on plasmid conjugative transfer of Escherichia coli and its relationship with toxic effects on growth*. Ecotoxicology and Environmental Safety, 205, p.111300. https://doi.org/10.1016/j.ecoenv.2020.111300.

Lin, H.; Ning, X.; Wang, D.; et al. (2023): *Quorum-sensing gene regulates hormetic effects induced by sulfonamides in Comamonadaceae*. Applied and Environmental Microbiology, 89(12), p.e0166223. https://doi.org/10.1128/aem.01662-23.

Liu, H.; Li, S.; Zhang, S.; et al. (2024): *Sulfamethoxazole exposure shifts partial denitrification to complete denitrification: Reactor performance and microbial community*. Chemosphere, 364, p.143225. https://doi.org/10.1016/j.chemosphere.2024.143225.

Liu, Y.; Chen, S.; Zhang, J.; Li, X.; Gao, B. (2017): *Stimulation effects of ciprofloxacin and sulphamethoxazole in Microcystis aeruginosa and isobaric tag for relative and absolute quantitation-*

*based screening of antibiotic targets*. Molecular Ecology, 26(2), p.689–701. https://doi.org/10.1111/mec.13934.

McMurdie, P. J.; Holmes, S. (2013): *phyloseq: an R package for reproducible interactive analysis and graphics of microbiome census data*. PloS One, 8(4), p.e61217. https://doi.org/10.1371/journal.pone.0061217.

Musat, N.; Musat, F.; Weber, P. K.; Pett-Ridge, J. (2016): *Tracking microbial interactions with NanoSIMS*. Current Opinion in Biotechnology, 41, p.114–121. https://doi.org/10.1016/j.copbio.2016.06.007.

Musat, N.; Stryhanyuk, H.; Bombach, P.; et al. (2014): *The effect of FISH and CARD-FISH on the isotopic composition of (13)C- and (15)N-labeled Pseudomonas putida cells measured by nanoSIMS*. Systematic and Applied Microbiology, 37(4), p.267–276. https://doi.org/10.1016/j.syapm.2014.02.002.

Oksanen, J.; Simpson, G. L.; Blanchet, F. G.; et al. (2022): *vegan: Community Ecology Package. R package version 2.6-0*.

Ouyang, W.-Y.; Su, J.-Q.; Richnow, H. H.; Adrian, L. (2019): *Identification of dominant sulfamethoxazole-degraders in pig farm-impacted soil by DNA and protein stable isotope probing*. Environment International, 126, p.118–126. https://doi.org/10.1016/j.envint.2019.02.001.

Paumelle, M.; Donnadieu, F.; Joly, M.; Besse-Hoggan, P.; Artigas, J. (2021): *Effects of sulfonamide antibiotics on aquatic microbial community composition and functions*. Environment International, 146, p.106198. https://doi.org/10.1016/j.envint.2020.106198.

Pesce, S.; Kergoat, L.; Paris, L.; et al. (2021): *Contrasting Effects of Environmental Concentrations of Sulfonamides on Microbial Heterotrophic Activities in Freshwater Sediments*. Frontiers in Microbiology, 12, p.753647. https://doi.org/10.3389/fmicb.2021.753647.

Polerecky, L.; Adam, B.; Milucka, J.; et al. (2012): *Look@NanoSIMS--a tool for the analysis of nanoSIMS data in environmental microbiology*. Environmental Microbiology, 14(4), p.1009–1023. https://doi.org/10.1111/j.1462-2920.2011.02681.x.

Qi, M.; Liang, B.; Zhang, L.; et al. (2021): *Microbial Interactions Drive the Complete Catabolism of the Antibiotic Sulfamethoxazole in Activated Sludge Microbiomes*. Environmental Science and Technology, 55(5), p.3270–3282. https://doi.org/10.1021/acs.est.0c06687.

Ricken, B.; Corvini, P. F.; Cichocka, D.; et al. (2013): *Ipso-hydroxylation and subsequent fragmentation: a novel microbial strategy to eliminate sulfonamide antibiotics*. Applied and Environmental Microbiology, 79(18), p.5550–5558. https://doi.org/10.1128/AEM.00911-13.

Schuijt, L. M.; van Drimmelen, C. K.; Buijse, L. L.; et al. (2024): *Assessing ecological responses to exposure to the antibiotic sulfamethoxazole in freshwater mesocosms*. Environmental Pollution, 343, p.123199. https://doi.org/10.1016/j.envpol.2023.123199.

Schwarzenbach, R. P.; Escher, B. I.; Fenner, K.; et al. (2006): *The challenge of micropollutants in aquatic systems*. Science, 313(5790), p.1072–1077. https://doi.org/10.1126/science.1127291.

Straub, J. O. (2016): *Aquatic environmental risk assessment for human use of the old antibiotic sulfamethoxazole in Europe*. Environmental Toxicology and Chemistry, 35(4), p.767–779. https://doi.org/10.1002/etc.2945.

Stryhanyuk, H.; Calabrese, F.; Kümmel, S.; et al. (2018): *Calculation of Single Cell Assimilation Rates From SIP-NanoSIMS-Derived Isotope Ratios: A Comprehensive Approach*. Frontiers in Microbiology, 9, p.2342. https://doi.org/10.3389/fmicb.2018.02342.

Sun, H.; Chen, R.; Jiang, W.; Chen, X.; Lin, Z. (2019): *QSAR-based investigation on antibiotics facilitating emergence and dissemination of antibiotic resistance genes: A case study of sulfonamides against mutation and conjugative transfer in Escherichia coli*. Environmental Research, 173, p.87–96. https://doi.org/10.1016/j.envres.2019.03.020.

Švara, V.; Krauss, M.; Michalski, S. G.; et al. (2021): *Chemical Pollution Levels in a River Explain Site-Specific Sensitivities to Micropollutants within a Genetically Homogeneous Population of Freshwater Amphipods*. Environmental Science and Technology, 55(9), p.6087–6096. https://doi.org/10.1021/acs.est.0c07839.

Välitalo, P.; Kruglova, A.; Mikola, A.; Vahala, R. (2017): *Toxicological impacts of antibiotics on aquatic micro-organisms: A mini-review*. International Journal of Hygiene and Environmental Health, 220(3), p.558–569. https://doi.org/10.1016/j.ijheh.2017.02.003.

Vasconcelos, E. C. de; Dalke, C. R.; Oliveira, C. M. de (2017): *Influence of Select Antibiotics on Vibrio fischeri and Desmodesmus subspicatus at µg L-1 Concentrations*. Environmental Management, 60(1), p.157–164. https://doi.org/10.1007/s00267-017-0841-4.

Vesterlund, S.; Paltta, J.; Karp, M.; Ouwehand, A. C. (2005): *Measurement of bacterial adhesion-in vitro evaluation of different methods*. Journal of Microbiological Methods, 60(2), p.225–233. https://doi.org/10.1016/j.mimet.2004.09.013.

Vila-Costa, M.; Gioia, R.; Aceña, J.; et al. (2017): *Degradation of sulfonamides as a microbial resistance mechanism*. Water Research, 115, p.309–317. https://doi.org/10.1016/j.watres.2017.03.007.

Wang, J.; Wang, S. (2018a): *Microbial degradation of sulfamethoxazole in the environment*. Applied Microbiology and Biotechnology, 102(8), p.3573–3582. https://doi.org/10.1007/s00253-018-8845-4.

Wang, T.; Wang, D.; Lin, Z.; et al. (2016): *Prediction of mixture toxicity from the hormesis of a single chemical: A case study of combinations of antibiotics and quorum-sensing inhibitors with gram-negative bacteria*. Chemosphere, 150, p.159–167. https://doi.org/10.1016/j.chemosphere.2016.02.018.

Weitere, M.; Altenburger, R.; Anlanger, C.; et al. (2021): *Disentangling multiple chemical and non-chemical stressors in a lotic ecosystem using a longitudinal approach*. Science of the Total Environment, 769, p.144324. https://doi.org/10.1016/j.scitotenv.2020.144324.

Wilkinson, J. L.; Boxall, A. B.; Kolpin, D. W.; et al. (2022): *Pharmaceutical pollution of the world's rivers*. Proceedings of the National Academy of Sciences, 119(8). https://doi.org/10.1073/pnas.2113947119.

Xu, H.; Lu, G.; Xue, C. (2020): *Effects of Sulfamethoxazole and 2-Ethylhexyl-4-Methoxycinnamate on the Dissimilatory Nitrate Reduction Processes and N2O Release in Sediments in the Yarlung Zangbo River*. International Journal of Environmental Research and Public Health, 17(6). https://doi.org/10.3390/ijerph17061822.

Yergeau, E.; Sanschagrin, S.; Waiser, M. J.; Lawrence, J. R.; Greer, C. W. (2012): *Sub-inhibitory concentrations of different pharmaceutical products affect the meta-transcriptome of river biofilm communities cultivated in rotating annular reactors*. Environmental Microbiology Reports, 4(3), p.350–359. https://doi.org/10.1111/j.1758-2229.2012.00341.x.

You, R.; Sun, H.; Yu, Y.; et al. (2016): *Time-dependent hormesis of chemical mixtures: A case study on sulfa antibiotics and a quorum-sensing inhibitor of Vibrio fischeri*. Environmental Toxicology and Pharmacology, 41, p.45–53. https://doi.org/10.1016/j.etap.2015.10.013.

Zhang, Y.; Da He; Bu, Z.; et al. (2022): *The transcriptomic analysis revealed sulfamethoxazole stress at environmentally relevant concentration on the mechanisms of toxicity of cyanobacteria*

*Synechococcus sp*. Journal of Environmental Chemical Engineering, 10(3), p.107637. https://doi.org/10.1016/j.jece.2022.107637.

## Figures legends

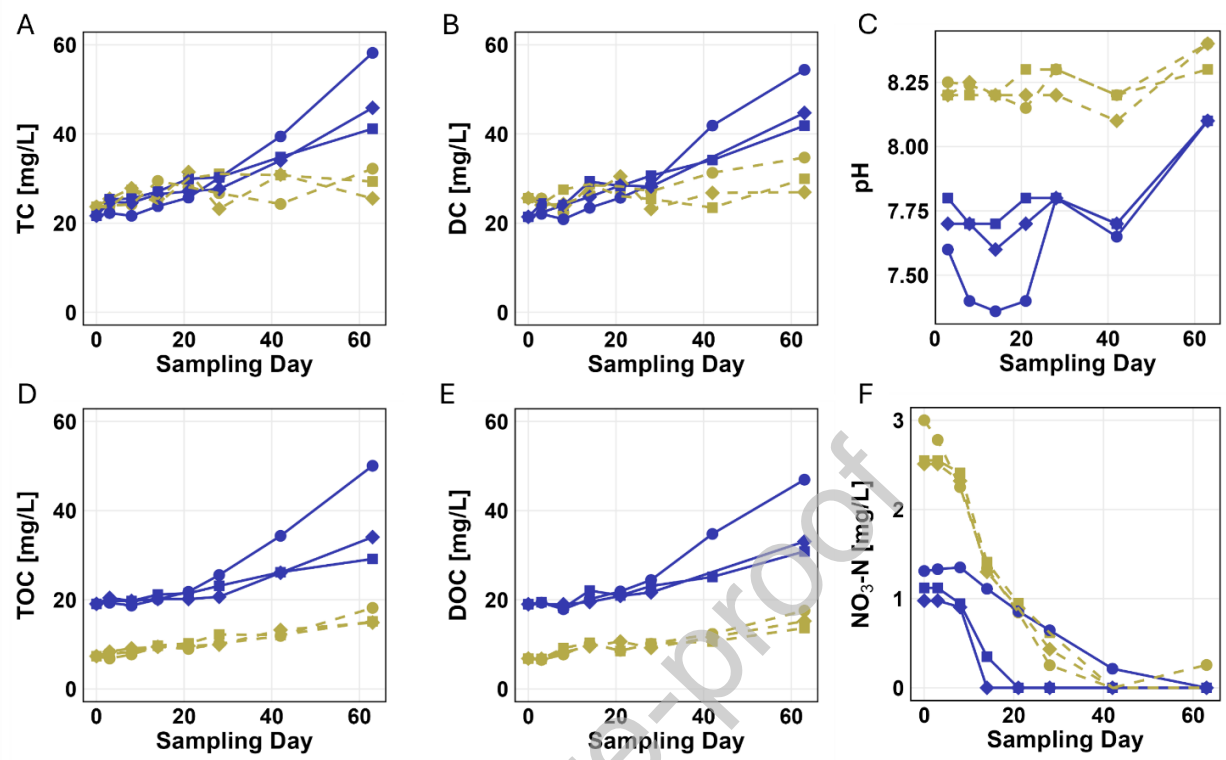


**Figure 1.** Physicochemical parameters in flume systems monitored over a time course of 63 days. (A) Total carbon (TC) concentration in mg/L. (B) Dissolved carbon (DC) concentration in mg/L. (C) pH. (D) Total organic carbon (TOC) concentration in mg/L. (E) Dissolved organic carbon (DOC) concentration in mg/L. (F) Nitrate concentration in mg/L. Colors and line type represent the river water (yellow, dashed line – wastewater-impacted water; blue, solid line – near-pristine water), the shape represents the type of SMX addition (circle – no SMX; square – $^{12}$C-SMX; diamond – $^{13}$C-SMX). Not shown are water temperature (17-19 °C during the operational period), oxygen saturation (always 102 %), ammonium and nitrite concentrations (always <0.1 mg/L, with no apparent differences between the systems).

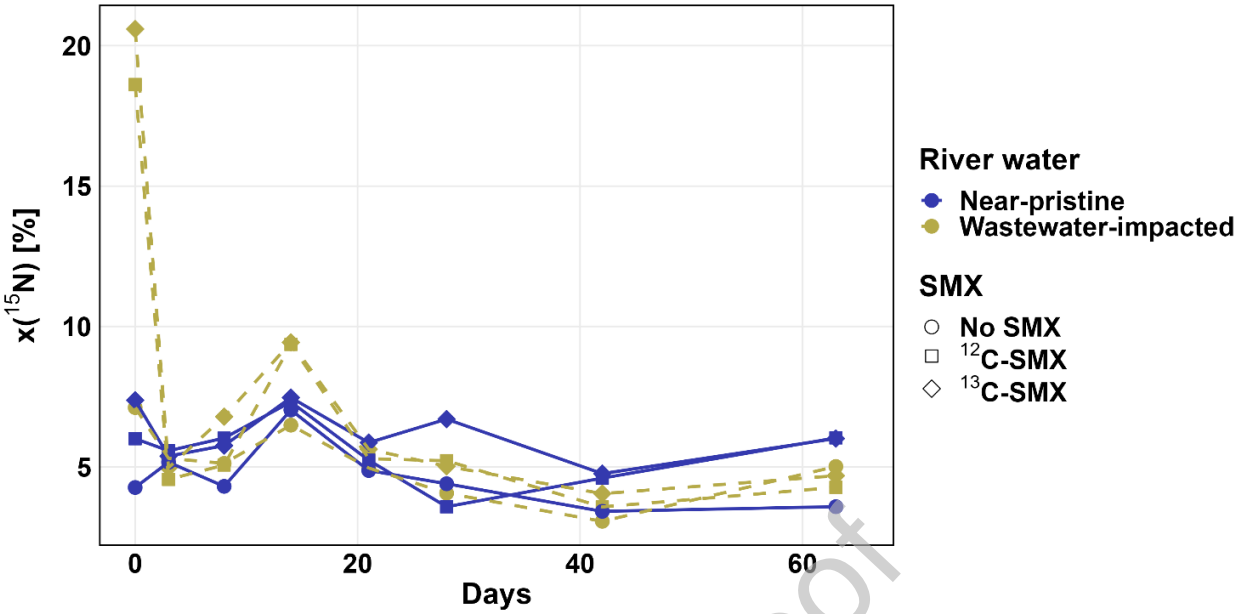


**Figure 2.** EA-IRMS measurements of $^{15}$N-uptake by bulk biomass in flume systems, expressed as $^{15}$N atom fraction over time. Colors and line types represent the sampling site (yellow, dashed line – wastewater impacted water; blue, solid line – near pristine water), shape represents the absence or addition of SMX (circle – no SMX; square – $^{12}$C SMX; diamond – $^{13}$C SMX).

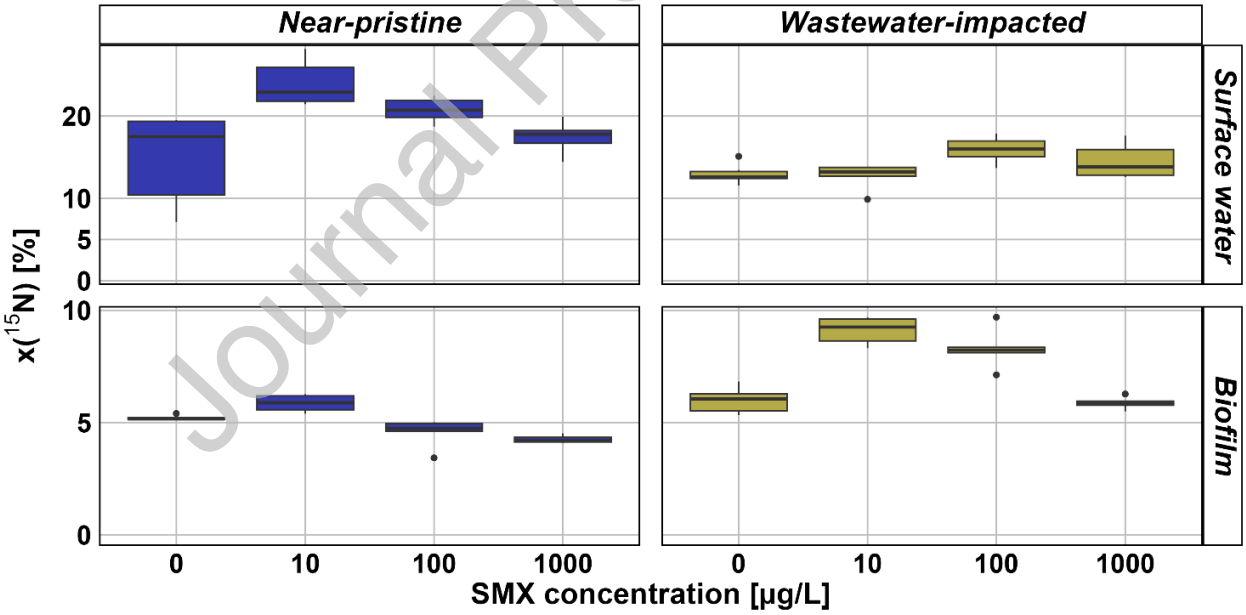


**Figure 3.** EA-IRMS measurements of $^{15}$N uptake by the bulk biomass in 24 h labelling experiments, shown for surface water (top) and biofilm samples (bottom). x($^{15}$N) [%] is the $^{15}$N isotope enrichment relative to natural abundance. Colors represent the sampling site (blue – near-pristine; yellow – wastewater-impacted). n=6 per condition.

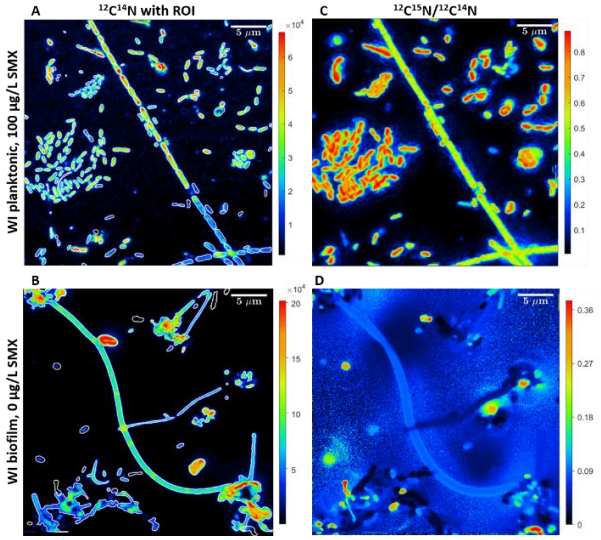


**Figure 4.** Representative chemical maps acquired during the nanoSIMS analysis showing the isotopic enrichment of biomass for a wastewater-impacted planktonic sample with 100 µg/L SMX (A and C) and a wastewater-impacted biofilm sample without SMX (B and D) after 24 h of incubation. (A and B) $^{12}C^{14}N^-$ to define regions of interest (displayed in white). The colorbar indicates the secondary ion counts per pixel. (C and D) $^{12}C^{15}N^-/^{12}C^{14}N^-$ for quantification of nitrogen assimilation. The colorbar indicates the ratio of $^{12}C^{15}N^-$ over $^{12}C^{14}N^-$.

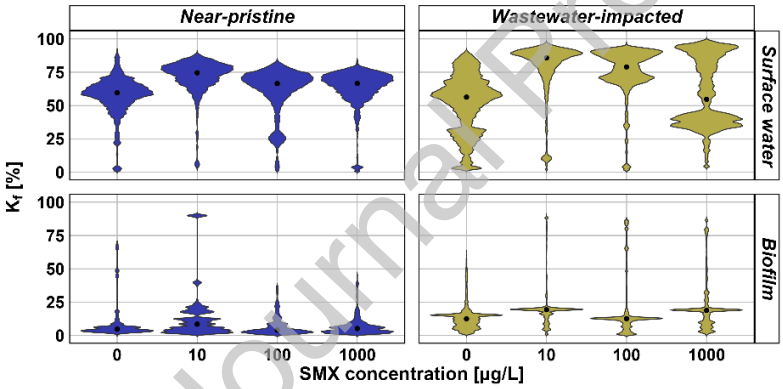


**Figure 5.** Distribution of $^{15}N$ assimilation ($K_f$) per pixel, derived from NanoSIMS measurements of selected regions of interest (ROI) in biomass from surface water (top) and biofilm compartment (bottom). Colors indicated the sampling site (blue – near-pristine; yellow – wastewater-impacted), the width of each violin plot represents the relative proportion of pixels corresponding to a given $^{15}N$ assimilation value within the respective ROI. Black dots display the median values.

## Graphical abstract

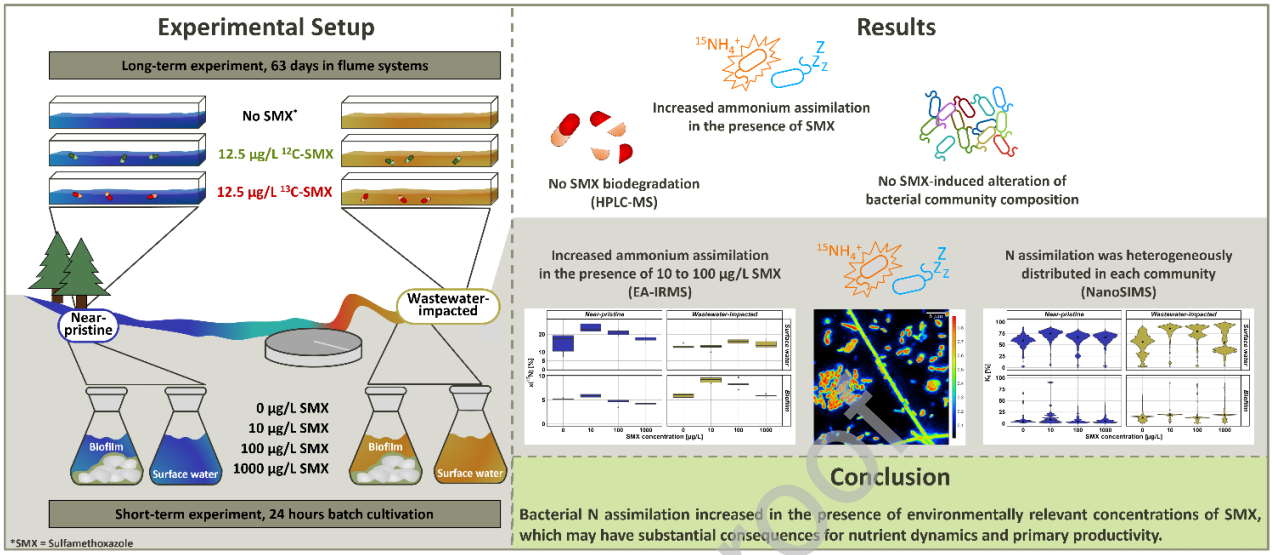


## Declaration of interests

☐ The authors declare that they have no known competing financial interests or personal relationships that could have appeared to influence the work reported in this paper.

☒ The authors declare the following financial interests/personal relationships which may be considered as potential competing interests:

| |
|---|
| Niculina Musat reports financial support was provided by Novo Nordisk Foundation. Co-author HHR is employed by Isodetect Umweltmonitoring GmbH (Leipzig, Germany). If there are other authors, they declare that they have no known competing financial interests or personal relationships that could have appeared to influence the work reported in this paper. |